*Proceedings of the Twenty-second (2012) International Offshore and Polar Engineering Conference*
*Rhodes, Greece, June 17–22, 2012*

*ISBN 978-1-880653-94–4 (Set); ISSN 1098-6189 (Set)*

**www.isope.org**

# Innovative Submerged Structures/Vegetation Effects on Coastal Erosion: Numerical Modeling of Hydro-Morphological Processes

*Th. Karambas, Ch. Koftis, E. Koutandos and P. Prinos*
*School of Civil Engineering, Aristotle University of Thessaloniki
Thessaloniki, Greece

## ABSTRACT

In the present work the application of an advanced hydro-morphological mathematical model for the design of innovative submerged structures for coastal protection, is presented.

Non linear wave transformation in the surf and swash zone is computed by a non-linear breaking wave model based on the higher order Boussinesq equations for breaking and non breaking waves.

The new Camenen and Larson (2007) transport rate formula involving unsteady aspects of the sand transport phenomenon is adopted for estimating the sheet flow sediment transport rates as well as the bed load and suspended load over ripples. Suspended sediment transport rate estimation is based on an exponential profile of sediment concentration for the steady equilibrium according to Camenen and Larson (2007, 2008).

The methodology is applied for the simulation of sediment transport and morphology evolution in coastal regions where innovative submerged structures/vegetation for coastal protection have been constructed. These structures and vegetation reduce the incident wave energy and consequently the wave erosive action.

KEY WORDS: Submerged structures, coastal erosion, vegetation, sediment transport, numerical models..

## INTRODUCTION

Over the past decades the problem of coastal erosion has expanded and there has been noted an important retreat of the shoreline. The solutions used to confront this problem until recently have been basically constituted of 'hard' conventional methods such as emerged breakwaters, seawalls, groynes. However, environmentally friendly coastal protection methods, such as submerged breakwaters and artificial reefs, have become nowadays increasingly popular. They can be considered as a 'soft' shore protection method, provided that it does not have optical harmful effect and mainly does not prevent significantly the circulation of waters, contrary to the conventional methods.

A proper design of the above methods requires the use of advanced mathematical models, able to simulate the complicated hydro-morphodynamic processes of the nearshore region (including swash zone), such as nonlinear wave propagation, wave-induced current, sediment transport by waves and currents and bed morphology evolution. The Boussinesq models and their combination with a sediment transport model seem to be suitable for the above purpose (Karambas and Koutitas, 2002, Karambas, 2002 & 2004, Karambas and Karathanassi, 2004). These models have the advantage that they can incorporate nonlinear breaking and non breaking irregular wave propagation from deep to shallow water and the swash zone. The models include the prediction of quasi-3D currents and long waves and provide to the sediment transport formulae all the required information such as, breaking wave induced turbulence, near bed velocity asymmetry and acceleration, swash zone modeling etc. (Karambas and Koutitas, 2002, Karambas, 2002 & 2004, Wenneker et al., 2011).

In the present work, the non linear wave transformation in the surf and swash zone is computed by a non-linear breaking wave model based on the higher order Boussinesq equations for breaking and non breaking waves. The Camenen and Larson (2005, 2007, 2008) transport rate formula involving unsteady aspects of the sand transport phenomenon is adopted for estimating bed load as well as and suspended load. The methodology is applied for the simulation of sediment transport and morphology evolution in coastal regions where innovative submerged structures (such as artificial reefs, bottom vegetation) for coastal protection have been constructed. These structures reduce the incident wave energy and consequently the wave erosive action. Some examples of innovative submerged structures are Reef Ball (Harris, 2009) and TECNOREEF (http://www.tecnoreef.com/).

## WAVE MODEL

### Boussinesq Model

A weakly nonlinear Boussinesq-type model with improved linear dispersion characteristics is used to describe wave motion in the regions upstream and downstream of the breakwater (Madsen and Sørensen, 1992). Above the breakwater the model incorporates two extra terms accounting for the interaction between the waves over the structure and the flow within the porous structure, one in the continuity equation and one in the momentum equation respectively, following the approach of Cruz et al. (1997). In one-dimensional form the governing equations (continuity and momentum equations) are:

$$\frac{\partial \eta}{\partial t}+\frac{\partial[(h+\eta)U]}{\partial x}+\varphi\frac{\partial(h_s\cdot U_s)}{\partial x}=0$$

$$\frac{\partial U}{\partial t}+U\frac{\partial U}{\partial x}+g\frac{\partial \eta}{\partial x} = \frac{h^2}{3}\frac{\partial^3 U}{\partial x^2\partial t}+(h+\eta)\frac{\partial h}{\partial x}\frac{\partial^3 U}{\partial x^2\partial t}$$
$$+Bh^2\left(\frac{\partial^3 U}{\partial x^2\partial t}+\frac{\partial^3 \eta}{\partial x^3}\right)+Bh\left(\frac{\partial^2 U}{\partial x\partial t}+\frac{\partial^2 \eta}{\partial x^2}\right)$$
$$+\varphi h\left(\frac{\partial h_s}{\partial x}\frac{\partial^2 U_s}{\partial x\partial t}+\frac{1}{2}h_s\frac{\partial^3 U_s}{\partial x^2\partial t}\right) \qquad (1)$$

where U = depth averaged horizontal velocity, $\eta$ = surface elevation, h = water depth, B = dispersion coefficient, $U_s$ = seepage (fluid) velocity inside the porous medium, $h_s$ = porous medium thickness and $\varphi$ = porosity.

The additional dispersion terms proportional to B extend the applicability of the model into a wider range of depths. As suggested by Madsen and Sørensen (1992), B is set equal to 1/15, value that gives the closest match to linear theory dispersion relation for $h/L_0$ as large as 0.5.

## Incorporation of bottom vegetation and artificial reefs

The effects of bottom vegetation and/or of artificial reefs are incorporated by solving the porous flow equations. Thus equations (1) (free surface flow model) are solved in the region of the breakwater in conjunction with a depth-averaged Darcy-Forchheimer (momentum) equation describing the flow inside the porous medium. Assuming that $O[(h_s/L)^2] << 1$ the momentum equation written in terms of the fluid velocity $U_s$ ($U_D = \varphi U_s$, $U_D$ = Darcy velocity) reduces to (Cruz et al., 1997, Gu andWang, 1991)

$$c_r\left(\frac{\partial U_s}{\partial t}+U_s\frac{\partial U_s}{\partial x}\right)+g\frac{\partial \eta}{\partial x}+\varphi\alpha_1 U_s+\varphi^2\alpha_2 U_s|U_s|=0 \qquad (2)$$

which is referred as the nonlinear long wave equation for porous medium. The third term in equation (2) is the Darcy term, while the fourth term is the Forchheimer term accounting for viscous and inertia forces respectively. In equation (2), $c_r$ = inertial coefficient, given by

$$c_r=\varphi+(1-\varphi)(1+c_m) \qquad (3)$$

where $c_m$ = added mass coefficient. $c_r$ is set equal to unity as recommended for porous media flow (Sollitt & Cross, 1976).

The porous resistance coefficients $\alpha_1$ and $\alpha_2$, are estimated from relationships given in Ward (1964), Sollitt & Cross (1972), Losada et al. (1995), Cruz et al. (1997).

## Wave breaking

An eddy viscosity formulation is adopted in order to simulate wave breaking (Kennedy et al., 2000) by introducing an eddy viscosity term in the right-hand-side of the momentum equation (1). This term is written (subscripts of x and t denote spatial and temporal differentiation respectively) as

$$E_{b_x}=\frac{1}{h+\eta}\{\nu_e[(h+\eta)U]_x\}_x \qquad (4)$$

The eddy viscosity $\nu_e$, is a function of both space and time and is given by

$$\nu_e = B\delta_b{}^2(h+\eta)\eta_t \qquad (5)$$

where $\delta_b$ = mixing length coefficient equal to 1.2. The quantity B controls the occurrence of breaking and varies from 0 to 1 as follows

$$B=\begin{cases}1, & \eta_t \ge 2\eta_t^*\\ \frac{\eta_t}{\eta_t^*}-1, & \eta_t^* < \eta_t \ge 2\eta_t^*\\ 0, & \eta_t \le \eta_t^*\end{cases} \qquad (6)$$

The parameter $\eta_t^*$ determines the onset and cessation of breaking and is defined as

$$\eta_t^*=\begin{cases}\eta_t^{(F)}, & t \ge T^*\\ \eta_t^{(I)}+\frac{t-t_0}{T^*}\left(\eta_t^{(F)}-\eta_t^{(I)}\right), & 0<t-t_0\ge T^*\end{cases} \qquad (7)$$

where $T^*$ = transition time $\left(=5\sqrt{g/h}\right)$, $t_0$ = time that breaking was initiated, and thus $t-t_0$ = age of the breaking event. The values of $\eta_t^{(I)}$ and $\eta_t^{(F)}$ are $0.35\sqrt{gh}$ and $0.15\sqrt{gh}$ respectively.

## Near bottom horizontal velocity

For breaking waves the horizontal velocity near the bottom is calculated according to Schaffer et al. (1993):

$$u_o=\frac{Uh-c\delta}{h+\eta-\delta} \qquad (8)$$

(3)

where c is the wave celerity and $\delta$ the roller thickness, which is determined geometrically.

For non breaking wave the parabolic distribution given by Peregrine (1972) is used.

(4)

## Bed friction effects

The instantaneous bottom shear stress is approximated using the formula:

$$\frac{\tau_b}{\rho}=\frac{1}{2}f_w u_o|u_o| \qquad (9)$$

where $u_o$ is the instantaneous bottom velocity) and $f_w$ is the bottom friction factor (Nielsen, 1992, chapter 3).

The term $-\tau_b/\rho h$ is included in the right hand side of the

momentum equation (1).

## Runup simulation

The 'dry bed' boundary condition is used to simulate runup. The condition, at the point i, is written:

if $(d+\zeta)_{i-1}$ <0.00001 m and $U_i$>0 then $\zeta_i = -d$ and $U_i = 0$

and

if $(d+\zeta)_i$ <0.00001 m and $U_i$<0 then $\zeta_i = -d$ and $U_i = 0$

which is very simple and very easily incorporated in a nonlinear wave model.

## Undertow calculation

The mean undertow $U_m$, as well as all the time mean values of the parameters, are obtained following the procedure proposed by Rakha et al. (1997) for irregular waves. The time series of the bottom velocities $u_o$ calculated by the wave model are divided into a number of cycles $N_c$ each consisting of $N$ time steps. All calculations described below are performed for each cycle separately. For each cycle the values of the bottom velocity $u_o$ are time averaged over $N$ time steps to obtain automatically the mean undertow $U_m$ under the roller. The final value is calculated by averaging the mean undertow for $N_c$ cycles. In the case of periodic waves $U_m$ is obtained by averaging the instantaneous bottom velocity $u_o$ over three wave periods.

The above method can not predict the near bed shoreward drift (steady streaming) generated by the phase shift in orbital motions due to bottom boundary layer mechanisms (viscosity effects). That shoreward transport more frequently occurs in the offshore regions. Inside the surf zone the phase shift mechanism is suppressed by both the developing turbulence and the undertow acting in the middle layer, and so the resulting near bed mass transport should be directed offshore. The present model incorporates the above mechanisms by calculating the near bottom undertow velocity $U_b$ from the analytical expression proposed by Putrevu and Svendsen (1993) which is valid inside and outside surf zone:

$$\frac{U_b}{\sqrt{g(d+\bar{\zeta})}} = \left( \frac{U_m}{\sqrt{g(d+\bar{\zeta})}} - \frac{A}{6} + \frac{\tau_{sb}(d+\bar{\zeta})}{2\rho\nu_{tz}\sqrt{g(d+\bar{\zeta})}} \right) (1+R_1)^{-1} \tag{10}$$

where $\bar{\zeta}$ is the mean water level (set-up), $U_m$ is the mean undertow velocity $U_m = \overline{u_o}$, (the overbar denotes time averaging) $\tau_{sb}$ is the steady streaming term, $\nu_{tz}$ is the eddy viscosity coefficient, and $A$, $R_1$ are coefficients given by Putrevu and Svendsen (1993).

The eddy viscosity coefficient outside the bottom boundary layer $\nu_{tz}$ is given by (Stive and deVriend, 1987):

$$\nu_{tz} = 0.025 \left(d+\bar{\zeta}\right) \left(\frac{\overline{D}}{\rho}\right)^{1/3} \tag{11}$$

where $D$ is the wave energy dissipation per unit area due to breaking $D = \rho g c \delta \beta_D$, with $\beta_D$ a function of the angle of inclination of the roller taken equal to 0.1, $\beta_D = 0.1$, as suggested by Madsen et al. (1997) and $\overline{D} = \overline{0.1 \rho g c \delta}$.

## Numerical scheme

The governing equations are finite-differenced utilizing a high-order predictor-corrector scheme that employs a third-order explicit Adams-Bashforth predictor step and a fourth-order implicit Adams-Moulton corrector step (Wei and Kirby, 1995). The corrector step is iterated until the desirable convergence is achieved. First order spatial derivatives are discretized to fourth-order accuracy.

## Wave generation

Input waves are introduced inside the computational domain by using a source function method, according to Wei et al. (1999)

SENDIMENT TRANSPORT MODULE

The mode of sediment movement on the coast is usually divided into bed load, suspended load and sheet flow transport. Different model concepts are being presently used for the prediction of each one, which range from empirical transport formulas to more sophisticated bottom boundary layer models.

In the present work, the bed load transport ($q_{sb}$) is estimated with a quasi-steady, semi-empirical formulation, developed by Camenen, and Larson, (2005, 2007, 2008) for an oscillatory flow combined with a superimposed current under an arbitrary angle:

$$\Phi_b = \frac{q_{sb}}{\sqrt{(s-1)gd_{50}^3}} = a_n \sqrt{\theta_{cw,net}}\, \theta_{cw,m} \exp\left( -b \frac{\theta_{cr}}{\theta_{cw}} \right) \tag{12}$$

where $s$ (= $\rho_s/\rho$) is the relative density between sediment ($\rho_s$) and water ($\rho$), $g$ the acceleration due to gravity, $d_{50}$ the median grain size, $a_w$, $a_n$ and $b$ are empirical coefficients (Camenen and Larson 2007), $\theta_{cw,m}$ and $\theta_{cw}$ the mean and maximum Shields parameters due to wave-current interaction, and $\theta_{cr}$ the critical Shields parameter for the inception of transport. The net Shields parameter $\theta_{cw,net}$ is given by:

$$\theta_{cw,net} = \left(1 - a_{pl,b}\right)\theta_{cw,on} - \left(1 + a_{pl,b}\right)\theta_{cw,off} \tag{13}$$

where $\theta_{cw,on}$ and $\theta_{cw,off}$ are the mean values of the instantaneous Shields parameter over the two half periods $T_{wc}$ and $T_{wt}$ ($T_w = T_{wc} + T_{wt}$, in which $T_w$ is the wave period and $\alpha_{pl,b}$ a coefficient for the phase-lag effects (Camenen and Larson 2007).

The Shields parameter is defined by $\theta_{cw,j} = \frac{1}{2} f_{cw} U_{cw,j}^2 / \left[(s-1) g d_{50}\right]$, with $U_{cw}$ being the wave and current velocity $U_{cw} = u_o - \overline{u_o} + U_b$, $f_{cw}$ the friction coefficient taking into account wave and current interaction and the subscript j should be replaced either by *onshore* or *offshore*. For sediment transport estimation, we use the corrected near bottom $U_{cw}$ (which incorporates the effects of undertow) instead of the instantaneous bottom velocity $u_o$. The use of $U_{cw}$ also in (9) does not give any difference in wave hydrodynamics calculations.

Phase-lag effects in the sheet flow layer were included through the

coefficient (Camenen and Larson, 2007) with:

$$a_{pl} = a_{onshore} - a_{offshore}$$
$$a_j = \frac{v^{0.25} U_{wj}^{0.5}}{w_s T_j^{0.75}} \exp\left[ -\left( \frac{U_{w,crsf}}{U_{wj}} \right)^2 \right] \quad (14)$$

where $v$ is the kinematic viscosity of water, $U_{w\,crsf}$, the critical velocity for the inception of sheet flow, $U_w$ is the wave orbital velocity amplitude, $W_s$ the sediment fall speed and the subscript j should be replaced either by *onshore* or *offshore*.

Suspended sediment transport rate estimation is based on an exponential profile of sediment concentration for the steady equilibrium, according to Camenen and Larson (2007, 2008). The suspended sediment load ($q_{ss}$) is thus obtained from:

$$q_{ss,w} = U_{cw,net} \frac{c_R \varepsilon}{W_s} \left[ 1 - \exp\left( -\frac{w_s h}{\varepsilon} \right) \right] \quad (15)$$

where $c_R$ is the reference concentration at the bottom, ε the sediment diffusivity ( $\varepsilon = \nu_{tz}$ ), and $U_{cw,net}$, the net mean current $U_{cw,net} = U_m$.

The bed reference concentration is written as follows based on the analysis of a large data set on sediment concentration profiles (Camenen and Larson, 2007):

$$c_R = 3.51^{-3} \exp(-0.3 d_*) \theta_{cw,m} \exp\left( -4.5 \frac{\theta_{cr}}{\theta_{cw}} \right) \quad (16)$$

where $d_* = \sqrt[3]{(s-1) g / v^2}\, d_{50}$ is the dimensionless grain size.

Phase-lag effect in the suspended concentration due to ripples, is also incorporated according to Camenen and Larson (2007).

## COMPARISON WITH EXPERIMENTS: WAVE DAMPING OVER POSIDONIA OCEANICA MEADOW

The wave model is confirmed against large-scale experiments on wave damping over Posidonia Oceanica meadow (Koftis et al., 2011). The experiments were carried out in the CIEM wave flume (Canal d'Investigació i Experimentació Marítima) at the Universitat Polytecnica de Catalunya, Barcelona. The CIEM wave flume is 100 m long, 5 m deep and 3 m wide, capable of reproducing experiments in a prototype scale. The waves are generated by a wave paddle at the left side of the flume, and a sandy slope beach of 1:15 was formed at the opposite end, for the elimination of wave reflection. A 20 m long horizontal and flat sandy area was created in the central part of the flume and the patch of artificial *P. oceanica* with length L= 10.70 m was placed above, as shown in Figure 1.

The physical properties of the plant, such as the density and stiffness, are important in order to study the wave interaction, the bending of the leaves and the resulting wave damping efficiently. A typical physical *P. oceanica* stem is composed of four to eight ribbon-like leaves, each of them 1 cm wide, 1 mm thick and up to 1 m long. The density of the prototype plant, $\rho_S$ , ranges from 800 to 1200 kg/m$^3$ and the modulus of elasticity, E, ranges from 0.41 to 0.53 GPa as found in Folkard et al. (2005). The plant's stem density can vary from sparse (<150 stems/m$^2$) found in deeper waters to dense (>700 stems/m$^2$). The geometry of the artificial plant was chosen in order to reproduce that of the prototype one. Each stem of the artificial plant was composed of four leaves with 1cm width and 1mm thickness and variable leaf length; one pair of 35 cm long leaves, and another pair of 55 cm length. The leaves were inserted in a stiff 10.0 cm long rod, made of PVC, which was then placed in a metal board forming the artificial meadow (Fig. 2). Two different stem density patterns were chosen; a high density configuration with N = 360 stems/m$^2$, representative of a very dense Posidonia meadow patch and an average one, with N = 180 stems/m$^2$.

A series of experiments were performed for irregular waves propagating over the artificial *P. Oceanica* patch in intermediate and shallow waters. The wave conditions were selected in order to reproduce mild wave conditions of the Mediterranean Sea where *P. oceanica* is mainly found. Jonswap spectrum, with a γ parameter equal to 3.3, was used for the generation of irregular waves with the significant wave height $H_s$ ranging from 0.28 m to 0.40 m, the peak wave period $T_p$ from 2.0 s to 4.5 s. The water depth in the flume, next to the meadow, h ranged between 1.10 and 1.70 resulting in a range of the submergence ratio α (= $h_s$/h) from 0.32 to 0.50.

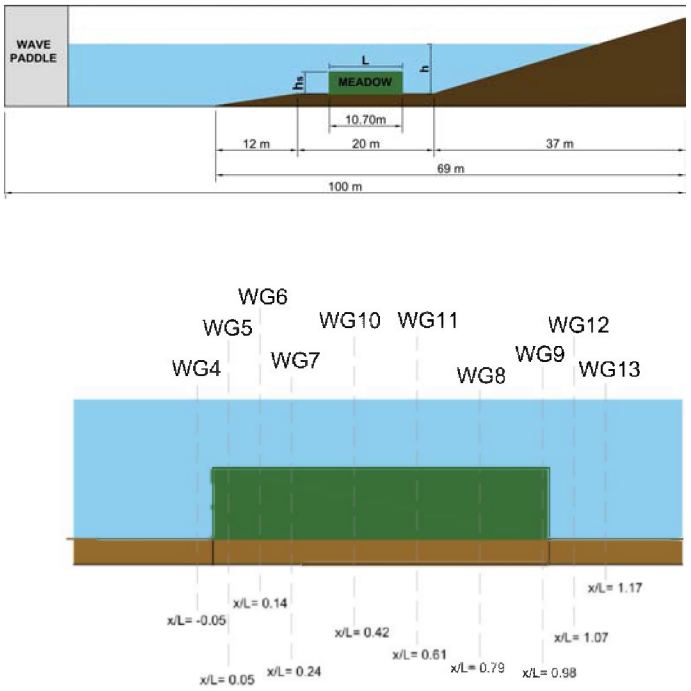


Figure 1. Sketch of the experimental setup of the CIEM flume and location of wave gauges.

The physical properties of the plant are incorporated in the porous flow model through three parameters: the porosity $\varphi$ and the porous resistance coefficients $\alpha_1$ and $\alpha_2$.

Two tests are reproduced:
Experiment 85 (significant wave height $H_s$=0.31 m, peak period $T_p$=4.0 sec, Water depth at meadow= 1.3m, Meadow height $h_s$=0.55m, Plant

density 180 stems/m$^2$) and Experiment 26 (significant wave height $H_s$=0.4 m, peak period $T_p$=3.0 sec, Water depth at meadow= 1.3m, Meadow height $h_s$=0.55m, Plant density 360 stems/m$^2$).

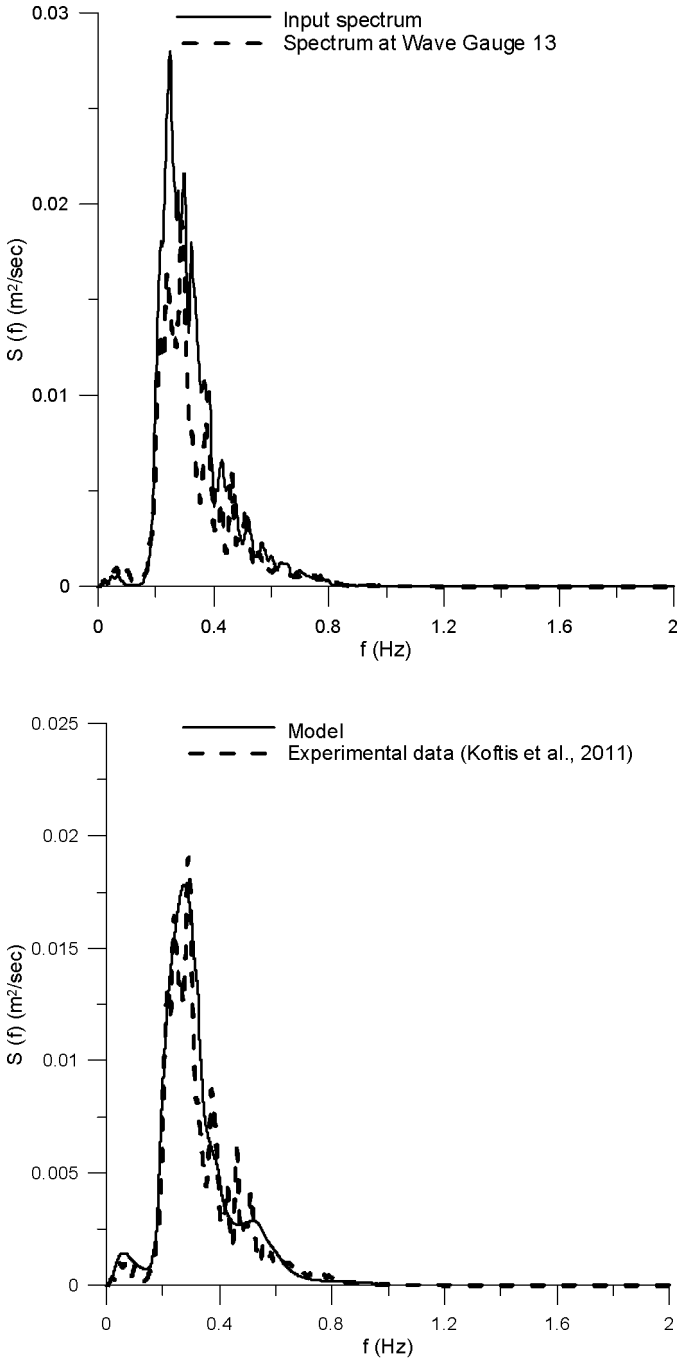


Figure 2. Input spectrum (top) and comparison of measured and calculated wave spectra at Wave Gauge 13 (bottom). Exp. 85, $H_s$=0.31 m, $T_p$=4.0 sec, Water depth at meadow= 1.3m, Meadow height $h_s$=0.55m, Plant density 180 stems/m$^2$.

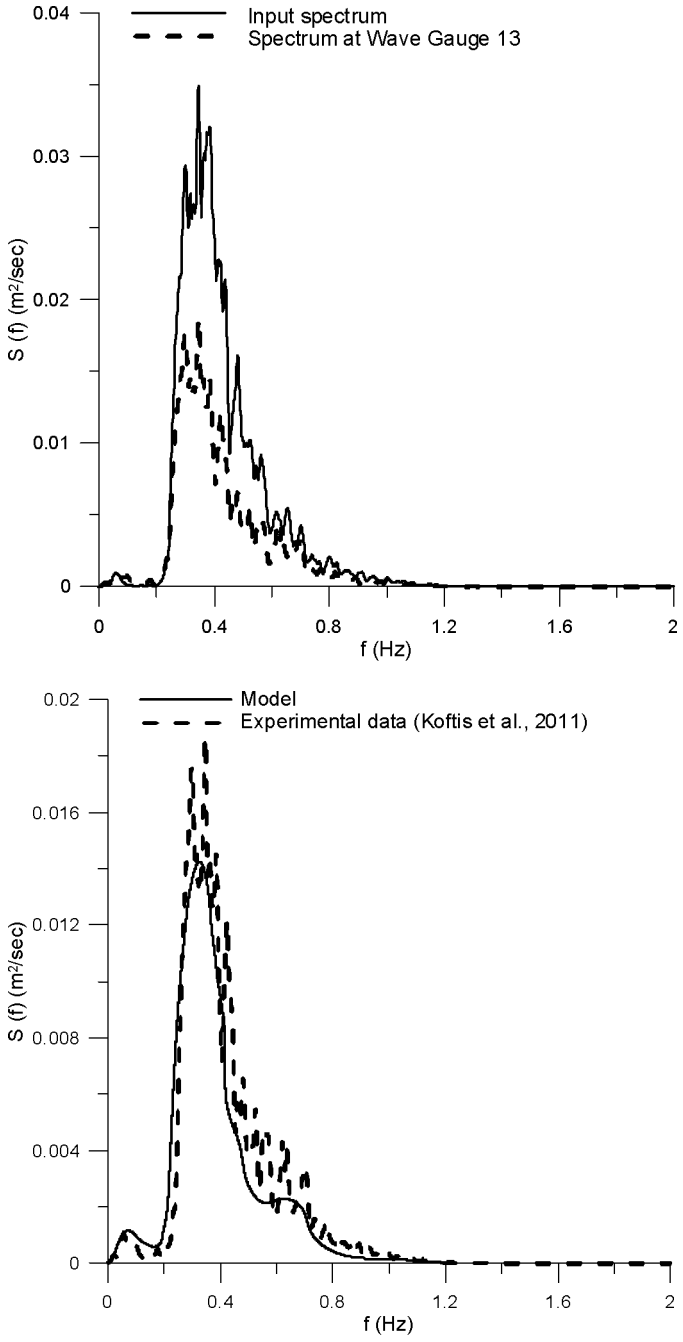


Figure 3. Input spectrum (top) and comparison of measured and calculated wave spectra at Wave Gauge 13 (bottom). Exp. 26, Hs=0.4 m, Tp=3.0 sec, Water depth at meadow= 1.3m, Meadow height $h_s$=0.55m, Plant density 360 stems/m$^2$.

The values of the porous resistance coefficients are: $\alpha_1 = 1$ and $\alpha_2 = 60$ for the experiment 85 (plant density 180 stems/m$^2$) and $\alpha_1 = 2.5$ and $\alpha_2 = 90$ for the experiment 26 (plant density 360 stems/m$^2$). The porosity is considered equal to 0.86 and 0.8 respectively, i.e $\varphi$**=0.86** for the experiment 85 and $\varphi$**=0.8** for the experiment 26. The above values of the porosity and the porous

resistance coefficients $\alpha_1$ and $\alpha_2$, are in accordance with the relationships given in the literature (Ward, 1964, Sollitt & Cross, 1972), Losada et al., 1995), Cruz et al., 1997) considering the physical properties of the plant, i.e. dimensions and plant's stem densities .

In Figure 2 and 3 the input wave spectra as well as the comparisons of measured and calculated wave spectra are shown. The comparison refers to Wave Gauge 13 (immediately downstream the vegetation). The effects of *Posidonia oceanica* meadows on the wave height damping is well simulated, while it can be concluded that the reduction of wave energy occurs without significant nonlinear wave-wave interactions and consequently without significant changes in the shape of the wave spectrum.

## APPLICATION TO CROSS-SHORE COASTAL EROSION

In this paragraph the model is applied to estimated innovative submerged structures effects on cross-shore sediment transport and beach morphology evolution.

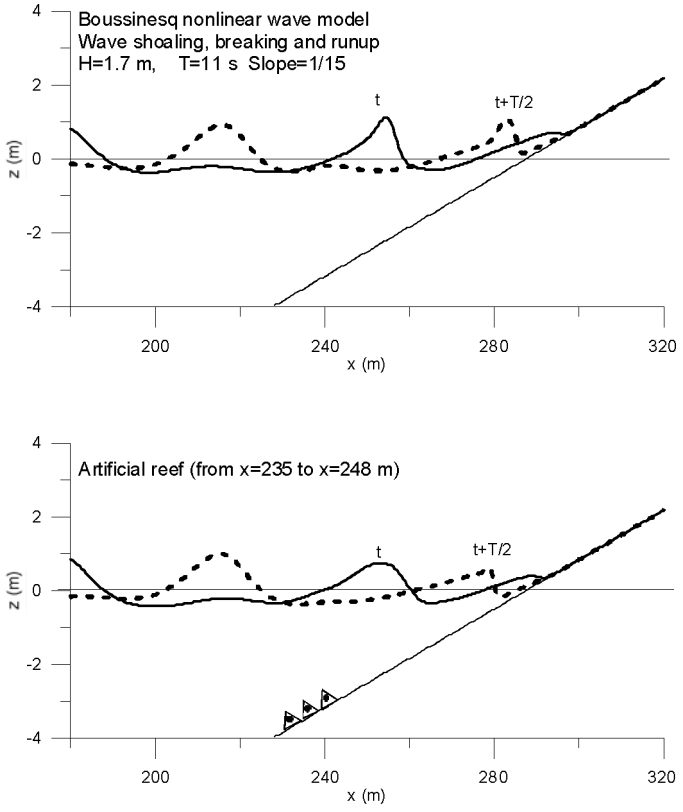


Figure 4. Shoaling, breaking, propagation and runup of regular wave with or without submerged structures ('Reef Ball' type artificial reef).

In figure 4 shoaling, breaking, propagation and run-up of regular waves on a 1/15 slope, with and without the presence of a artificial reef, is shown (Wave height H=1.7 m, period T=11 sec). The transmission coefficient is about 0.6 ($K_t$≈0.6). The transmission coefficient is defined as the ratio of the transmitted wave height to the incident wave height. With the presence of artificial reef, the incident wave height is reduced, and consequently breaking occurs closer to the shore line resulting to milder hydrodynamics conditions within the surf and swash zone.

The presence of the 'Reef Ball' type artificial reef is incorporated in the porous flow model through three parameters: the porosity $\varphi$ and the porous resistance coefficients $\alpha_1$ and $\alpha_2$. The values are calibrated to give a transmission coefficient equal to 0.6.

In Figure 5 cross-shore morphology evolution after 6 hr of wave action is shown. In the numerical experiment a grain size of $d_{50}$=0.22 mm is considered It is obvious that despite the relatively large value of the transmission coefficient, when artificial reef is present ($K_t$≈0.6), the reduction of the erosion is obvious. Notice that a transmission coefficient $K_t$≈0.6 corresponds to 36% wave energy transmission. This energy reduction seems to be quite significant.

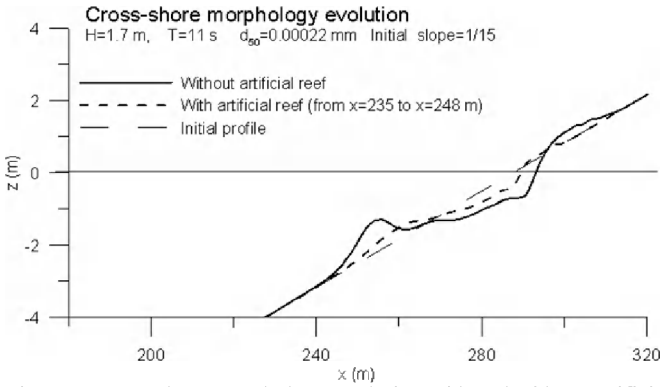


Figure 5. Cross-shore morphology evolution with and without artificial reef.

## CONCLUSIONS

- Using a coupled free-surface and porous flow model the effects of *Posidonia oceanica* meadows on the wave height damping is well simulated.
- Artificial reef and bottom vegetation result to relatively large values of transmission coefficients. However their effects on the reduction of coastal erosion is obvious.

## ACKNOWLEDGEMENTS

The support of the European Commission through FP7.2009-1, Contract 244104 – THESEUS (Innovative technologies for safer European coasts in a changing climate), is gratefully acknowledged.

## REFERENCES

Camenen, B., Larson, M. (2005), "A general formula for non-cohesive bed load sediment transport", *Estuarine, Coastal and Shelf Science* 63, 249-260.

Camenen, B., Larson, M. (2007). "A unified sediment transport formulation for coastal inlet application", *Technical report ERDC/CHL CR-07-1*, US Army Engineer Research and Development Center, Vicksburg, MS.

Camenen, B., Larson, M. (2008). "A general formula for noncohesive

suspended sediment transport", *Journal of Coastal Research* 24(3), 615-627.

Cruz, E. C., Isobe, M., Watanabe, A., (1997). "Boussinesq equations for wave transformation on porous beds". *Coastal Engineering*, 30, 125-156.

Gu, Z., Wang, H. (1991). "Gravity waves over porous bottoms". *Coastal Engineering*, 15, 497-524.

Harris L.E. (2009) "Artificial Reefs for Ecosystem Restoration and Coastal Erosion Protection with Aquaculture and Recreational Amenities". *Reef Journal*, Vol. 1 No. 1, pp. 235-246.

Karambas (2006). "Prediction of sediment transport in the swash zone by using a nonlinear wave model", *Continental Shelf Research*, 26, pp. 599-609.

Karambas Th. V. (2002). "Nonlinear Wave Modeling and Sediment Transport in the Surf and Swash Zone", *ADVANCES in COASTAL MODELING*, Elsevier Science Publishers.

Karambas Th. V. and C. Koutitas (2002). "Surf and swash zone morphology evolution induced by nonlinear waves", *Journal of Waterway, Port, Coastal and Ocean Engineering*, American Society of Civil Engineers, Vol. 128, no 3, pp. 102-113.

Karambas Th. V. and E.K. Karathanassi (2004). "Boussinesq modeling of Longshore currents and sediment transport", *Journal of Waterway, Port, Coastal and Ocean Engineering*, American Society of Civil Engineers, Vol. 130, no 6, pp. 277-286.

Kennedy, A.B., Chen, Q., Kirby, J.T., Darlymple, R.A. (2000). "Boussinesq modeling of wave transformation, breaking, and runup. I : 1D". *Journal of Waterway, Port, Coastal and Ocean Engineering* 121 (5), 251-261.

Koftis Th. , P. Prinos and V. Stratigaki (2011) "A large-scale experimental study on wave damping over Posidonia Oceanica meadow", THESEUS report (Innovative technologies for safer European coasts in a changing climate), EU FP7 PROGRAMME.

Liu, P. L.-F., Wen, J. (1997). "Nonlinear diffusive surface waves in porous media". *Journal of Fluid Mechanics*, 347, 26, 119-139.

Losada, I. J., Losada, M. A., Martín, A. (1995). "Experimental study of wave-induced flow in a porous structure". *Coastal Engineering*, 26, 77-98.

Losada, I. J., Silva, R., Losada, M. A. (1996). "3-D non-breaking regular wave interaction with submerged breakwaters". *Coastal Engineering*, 28, 229-248.

Madsen, P. A., (1974). "Wave transmission through porous structures". *Journal of Waterway, Harbour, Coastal and Ocean Engineering*, Div., ASCE, 100 (3), 169-188.

Madsen, P.A., Sørensen, O.R. (1992). "A new form of the Boussinesq equations with improved linear dispersion characteristics. Part 2: A slowly varying bathymetry". *Coastal Engineering*, 18, 183-204.

Madsen P., Sorensen O. and Schaffer H. (1997). "Surf zone dynamics simulated by a Boussinesq type model. Part I. Model description and cross-shore motion of regular waves." *Coastal Engineering*, 32, pp 255-287.

Nielsen, P. (1992). "Coastal Bottom Boundary Layers and Sediment Transport. " Advanced Series on Ocean Engineering, vol. 4. Word Scientific.

Peregrine, D.H. (1972.) "Equations for water waves and the approximation behind them." *Waves on Beaches and Resulting Sediment Transport*, ed. R. E. Meyer, Academic Press.

Putrevu U. and Svendsen I. A. (1993). "Vertical structure of the undertow outside the surf zone." *Journal of Geophysical Research*, vol. 98, no C12, pp. 22707-22716

Rakha K. A., Deigaard R. and Broker I. (1997). "A phase-resolving cross shore transport model for beach evolution." *Coastal Engineering*, 31, pp 231-261.

Schäffer H. A., Madsen P.A. and Deigaard R. (1993), "A Boussinesq model for waves breaking in shallow water", *Coastal Engineering*, 20, pp. 185-202.

Sollitt, C. K., Cross, R. H., (1972). "Wave transmission through permeable breakwaters". *Proceedings of 13th International Conference on Coastal Engineering*, ASCE, New York, 1827-1846.

Sollitt, C. K., Cross, R. H. (1976). "Wave reflection and transmission at permeable breakwaters". Technical Paper No. 76-8, CERC.

van Gent, M. R. A. (1994). "The modelling of wave action on and in coastal structures". *Coastal Engineering*, 22, 311-339.

de Vriend H. J. and Stive M. J. F. (1987). "Quasi-3D modelling of nearshore currents." *Coastal Engineering* 11, pp. 565-601.

Ward, J. C. (1964). "Turbulent flow in porous media. " *Journal of Hydraulic Division*, ASCE, 90 (HY5), 1-12.

Wei G., Kirby, J.T., Sinha, A. (1999). "Generation of waves in Boussinesq models using a source function method". *Coastal Engineering*, 36, 271-299.

Wei, G., Kirby, J.T. (1995). "Time-dependent numerical code for extended Boussinesq equations". *Journal of Waterway, Port, Coastal and Ocean Engineering*, 121 (5), 251-261.

Wenneker I., Ap van Dongeren, J. Lescinski, D. Roelvink, M. Borsboom (2011), "A Boussinesq-type wave driver for a morphodynamical model to predict short-term morphology", *Coastal Engineering* , 58, pp. 66–84.